AUTOPHAGY
2016, VOL. 12, NO. 11, 1984–1999
http://dx.doi.org/10.1080/15548627.2016.1208887

Taylor & Francis
Taylor & Francis Group

BASIC RESEARCH PAPER

Selective endosomal microautophagy is starvation-inducible in *Drosophila*

Anindita Mukherjee[a], Bindi Patel[a], Hiroshi Koga[a], Ana Maria Cuervo[a,b,c], and Andreas Jenny[a,b,c,d]

[a]Department of Developmental and Molecular Biology, Albert Einstein College of Medicine, New York, NY, USA; [b]Institute for Aging Studies, Albert Einstein College of Medicine, New York, NY, USA; [c]Marion Bessin Liver Research Center, Albert Einstein College of Medicine, New York, NY, USA; [d]Department of Genetics, Albert Einstein College of Medicine, New York, NY, USA

ABSTRACT

Autophagy delivers cytosolic components to lysosomes for degradation and is thus essential for cellular homeostasis and to cope with different stressors. As such, autophagy counteracts various human diseases and its reduction leads to aging-like phenotypes. Macroautophagy (MA) can selectively degrade organelles or aggregated proteins, whereas selective degradation of single proteins has only been described for chaperone-mediated autophagy (CMA) and endosomal microautophagy (eMI). These 2 autophagic pathways are specific for proteins containing KFERQ-related targeting motifs. Using a KFERQ-tagged fluorescent biosensor, we have identified an eMI-like pathway in *Drosophila melanogaster*. We show that this biosensor localizes to late endosomes and lysosomes upon prolonged starvation in a KFERQ- and Hsc70-4- dependent manner. Furthermore, fly eMI requires endosomal multivesicular body formation mediated by ESCRT complex components. Importantly, induction of *Drosophila* eMI requires longer starvation than the induction of MA and is independent of the critical MA genes *atg5, atg7*, and *atg12*. Furthermore, inhibition of Tor signaling induces eMI in flies under nutrient rich conditions, and, as eMI in *Drosophila* also requires *atg1* and *atg13*, our data suggest that these genes may have a novel, additional role in regulating eMI in flies. Overall, our data provide the first evidence for a novel, starvation-inducible, catabolic process resembling endosomal microautophagy in the *Drosophila* fat body.

ARTICLE HISTORY
Received 3 March 2015
Revised 15 June 2016
Accepted 27 June 2016

KEYWORDS
autophagy; chaperone-mediated autophagy; *Drosophila*; endosomal microautophagy; proteostasis; Tor

Introduction

Autophagy is an evolutionarily conserved catabolic process that mediates delivery of cytoplasmic components (proteins and organelles) to lysosomes for degradation and recycling.[1-3] Autophagic turnover is crucial for cell survival, differentiation, development, and energy homeostasis.[1,2,4,5] Autophagy protects cells by clearing damaged organelles and dysfunctional, misfolded or aggregated proteins, and also provides an adaptive response to various cellular stressors including starvation, proteotoxicity, lipotoxicity, and oxidative stress.[1] Not surprisingly, autophagy is increasingly implicated in counteracting various human pathologies including neurodegenerative disorders, infectious diseases, and cancer.[5,6] Furthermore, genetic experiments show that diminished autophagy accelerates aging-like phenotypes, whereas increased autophagy can extend life span.[7-9]

Three basic forms of autophagy have been identified in mammals: Macroautophagy (MA), microautophagy (MI), and chaperone-mediated autophagy (CMA).[5,10-12] During MA, the phagophore, a double-membrane structure, forms de novo and engulfs portions of cytoplasm including proteins and organelles; the phagophore subsequently matures into a closed autophagosome. Initiation of autophagosome formation requires activation of the Atg1-Atg13 and the Vps34-Vps30/Beclin 1 complexes. Elongation of the phagophore is then attained by 2 conjugation steps that depend on the E1-like enzyme Atg7: the formation of an Atg12–Atg5 conjugate[13] and lipidation of orthologs of yeast Atg8, such as the ubiquitin-like protein family MAP1LC3/LC3 (microtubule-associated protein 1 light chain 3).[14,15] After phagophore closure to form the autophagosome, the sequestered cytosolic contents are degraded upon fusion with lysosomes. Although macroautophagy can be highly selective for the degradation of specific organelles, pathogens and protein aggregates, degradation of soluble cytosolic proteins via macroautophagy occurs predominantly "in bulk." In contrast, CMA selectively degrades cytosolic proteins containing a motif biochemically related to KFERQ.[16] During CMA, the KFERQ-motif of the substrate protein is recognized by the cytosolic chaperone HSPA8 (heat shock protein family A [Hsp70] member 8, the mammalian ortholog of the *Drosophila* family of Hsc70 proteins),[17] which delivers them to LAMP2A (lysosomal-associated membrane protein 2A),[18] the limiting factor of CMA. Upon unfolding, the substrates translocate across the lysosomal membrane and are degraded.[19,20]

Endosomal microautophagy (eMI) has recently been identified in mammals[21] as a process whereby endosomes engulf cytosolic material through the formation of multivesicular bodies (MVBs) which is then degraded in late endosomes or upon their fusion with lysosomes. Cytosolic proteins degraded through eMI can be sequestered in bulk with other cytosolic components, or, if bearing a KFERQ motif, can be selectively

CONTACT Andreas Jenny andreas.jenny@einstein.yu.edu Albert Einstein College of Medicine, Chanin 503, 1300 Morris Park Ave., Bronx, NY 10461, USA.
Color versions of one or more of the figures in this article can be found online at www.tandfonline.com/kaup.
Supplemental data for this article can be accessed on the publisher's website.

targeted to this autophagy pathway. eMI thus shares molecular components with both the endocytic and the CMA pathways. Based on shRNA-mediated knockdown studies of TSG101 and VPS4,[21] it is demonstrated that eMI relies on the ESCRT (endosomal sorting complexes required for transport) machinery for endosome invagination and also requires HSPA8 for targeting of KFERQ-containing cargo.[21] In contrast to CMA, during which HSPA8 binds LAMP2A on lysosomes, cargo delivery by eMI requires HSPA8 binding to endosomal membrane phosphatidylserines and occurs independent of LAMP2A.[21] A form of microautophagy has also been described in yeast, whereby direct sequestration of cytosolic material occurs by small vesicles that form at the surface of the vacuole.[12] However, yeast microautophagy-specific orthologs have not been identified in mammals.[22]

While most autophagy-related (*atg*) genes involved in MA were originally identified in yeast,[3] the core MA machinery is conserved throughout the animal kingdom.[23] In *Drosophila melanogaster*, MA occurs in the larval salivary gland, midgut and fat body in a developmentally regulated manner, but can also be induced by starvation or oxidative stress.[24-27]

The 2A splice isoform of LAMP2, the only isoform able to function in CMA, is lacking in genomes other than mammals and birds and, therefore, CMA is predicted to be restricted to those species.[18] Nevertheless, our sequence analysis has revealed the occurrence of KFERQ-like motifs in about 43% of the *Drosophila* proteome. Using a KFERQ motif fused to photoactivatable mCherry originally developed as a model substrate to study CMA in mammalian cells,[28] we identified and characterized a selective, eMI-like process in vivo in *Drosophila* that is distinct from MA. When expressed in the fat body, functionally related to the mammalian liver,[29,30] the biosensor accumulates in puncta in a starvation inducible and KFERQ motif-dependent manner. Significantly, *Drosophila* eMI is temporally and genetically different from MA, as it requires starvation longer than 12 h. and is independent of *atg5, atg7*, and *atg12*. Colocalization studies reveal that the biosensor partially overlaps with late endosomes and accumulates in lysosomes in a process that requires Hsc70-4 and ESCRT components. Interestingly, the requirement of *atg1* and *atg13*, 2 genes responsible for coupling MA to starvation downstream of the Tor pathway,[24,31,32] suggest that they may have a novel, analogous function for eMI. Indeed, pharmacological or genetic interference with Tor signaling is sufficient to induce reporter puncta formation under fed conditions. Our findings suggest that eMI is not limited to mammals and that in *Drosophila* eMI is starvation-inducible.

Results

Starvation induced and KFERQ motif-dependent formation of biosensor puncta

To address the existence of an MA-independent selective autophagy pathway in *Drosophila*, we developed transgenic flies expressing a photoactivatable (PA) KFERQ-PA-mCherry biosensor under the control of the *UAS-Gal4* system, allowing for tissue-specific expression (see Materials and Methods).[33] This sensor consists of the N-terminal 21 amino acids of bovine RNASE1/RNase A including its KFERQ-CMA targeting motif fused to PA-mCherry. This reporter has previously been used as a model substrate to track CMA in mammalian cells upon photoactivation with 405-nm light in pulse-chase types of experiments (Fig. S1A).[28] In mammalian cells, activation of CMA for example by prolonged starvation induces reporter relocalization from a diffuse, cytoplasmic distribution to puncta that colocalize with lysosomes, but not autophagosomes or endosomes.[28] We expressed the biosensor using *cg-Gal4* in the larval fat body, a tissue commonly used to study starvation-induced MA[27,31,34-37] and photoactivated living early 3rd instar larvae (L3). The photoactivated larvae were then transferred either to 20% sucrose (for starvation) or 20% sucrose solution supplemented with heat-killed yeast (as regular, fed diet) for 2, 4, 22 and 25-h.[27] Autophagosomes in the fat body first appear after 1 h of starvation and MA reaches its highest level at approximately 4 h of starvation, when most autophagosomes have fused with lysosomes to form larger puncta.[24,27] Under fed conditions at all time points tested (Figs. 1A and 1B for 4 h and 25 h, respectively), the reporter was diffusely localized throughout the cytoplasm with discrete puncta rarely detected. Intriguingly, upon starvation, and considerably later than activation of MA, KFERQ-reporter puncta were first detected 21 to 22 h post starvation (hps) and were most prominent at 25 hps (Fig. 1D for 25 h; enlargement shown in Fig. 1E; note that several independent transgenic insertions showed equivalent results; quantification of puncta under fed and starved conditions is shown in Fig. 1F). Importantly, after 4 h of starvation, when MA was shown to be highly active ([24, 27] and Fig. S2A), the biosensor was diffuse throughout the cytosol (Fig. 1C). No fluorescent signal was detected in transgenic larvae without photoactivation (Figs. S1B to B″). These data indicate that biosensor puncta formation is dependent on prolonged starvation. A more extensive time course including 36-h and 48-h starvation showed the total reporter signal decreases after 12 hps with only weak signal remaining at 48 hps (quantified in Fig. S1F). Consistently, puncta appear around 12 hps and peak at 25 hps (Fig. S1G). Importantly, quantification of total reporter signal at 4 hps and 25 hps showed that the decrease in signal is significantly faster under starvation conditions than under fed conditions (Fig. 1G), suggesting that starvation indeed induces reporter degradation.

To confirm that sensor puncta formation (>12-h starvation required) is truly temporally distinct from MA (1-h starvation sufficient for induction) and not simply due to a longer time required for sensor puncta than for autophagosomes to form, we performed refeeding experiments. Larvae that were photoactivated at t = 0 were starved for increasing amounts of time and then refed until analysis 25 h after photoactivation (see schematic in Fig. 1H), as we hypothesized that we should be able to chase the sensor into puncta upon brief starvation, if it simply took the sensor longer to form puncta. Neither 1 h nor 4 h of starvation are sufficient to detect puncta 25 h after photoactivation (Fig. 1I). Puncta formation required at least 12-h starvation and again was strongest at 25 hps (Fig. 1I; note that no puncta formed under fed conditions), demonstrating that reporter puncta formation is kinetically distinct from MA.

To test whether reporter puncta formation requires the KFERQ-targeting motif, we developed control transgenic lines expressing either PA-mCherry alone or a mutant biosensor

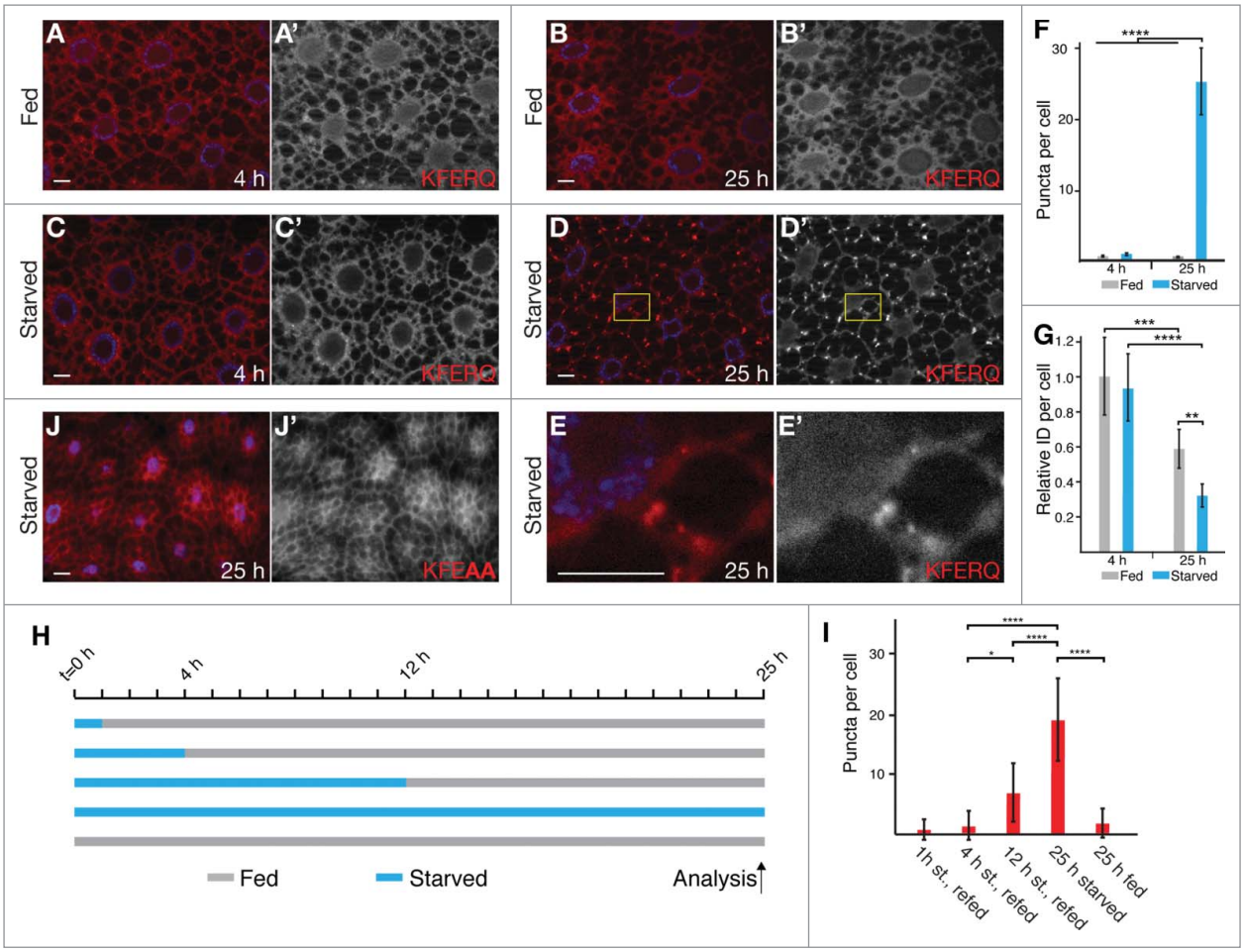

Figure 1. Sensor puncta formation upon prolonged starvation is KFERQ-motif-dependent. (A to E) Under fed conditions, the KFERQ-PAmCherry reporter signal is diffusely distributed in 3rd instar larval fat body cells 4 h (A) and 25 h (B) after photoactivation. Under starvation conditions, the sensor is mainly diffusely localized after 4 h post-starvation (hps; C), but shows a punctate pattern after prolonged starvation (25 hps; D). (E) Enlargement of area boxed in yellow in (D). (F) Quantification of puncta number per cell (see Materials and methods for details) at 4 hps and 25 hps under fed (gray bars) and starved (blue bars) conditions. n = 11 to 72 cells per genotype and time point. (G) Quantification of total reporter signal (Integrated Density, ID; normalized to 4 h fed) at 4 hps and 25 hps under fed (gray bars) and starved (blue bars) conditions. Importantly, the reporter signal disappears significantly faster under starvation, indicating reporter degradation. n = 11 to 66 cells per genotype and time point. (H and I) Reporter puncta formation requires prolonged starvation. (H) Schematic of refeeding experiment. After simultaneous photoactivation, larvae were separated and starved for the indicated amount of time (blue) and then refed (gray) for the remaining time until processing at 25 hps. (I) Quantification of KFERQ-PAmCherry reporter puncta per cell under the indicated conditions. Reporter puncta only start to form after at least 12 h of starvation and are very prominent by 25 hps, indicating that brief starvation is not sufficient to induce reporter degradation. n = 10 cells per condition. (J) A sensor with a mutated targeting motif (KFEAA) remains diffusely distributed even after prolonged starvation. In all figures, monochromatic (' and '') images show the indicated single channels. Nuclei are in blue in composite images. Areas devoid of any signal correspond to lipid droplets. ApoTome images; scale bars: 10 μm. One-way ANOVA $P < 0.0001$ with the Tukey post hoc test (*, $P < 0.05$; **, $P < 0.02$; ***, $P < 0.01$; ****, $P < 0.0001$).

with a nonfunctional KFEAA-sequence replacing the KFERQ-motif.[38,39] All sensor line expression levels were comparable (Fig. S1E). The mutant sensor (Fig. 1J) or PA-mCherry alone (Figs. S1C and S1D) remained diffusely localized in fat body cells and rarely showed puncta after prolonged starvation, indicating that reporter puncta formation depends on a functional KFERQ-motif. Dependence of sensor puncta on both a KFERQ-motif and prolonged starvation and their absence during the peak of MA suggests that the reporter puncta represent a novel selective autophagy pathway in flies.

Biosensor puncta colocalize with lysosomal and late endosomal markers

To characterize the biosensor puncta, we performed colocalization studies with respect to lysosomes, autophagosomes, and various endosome types. Coexpression of the reporter with UAS-GFP-HsLAMP1, a GFP fusion protein with a human LAMP1 fragment that is commonly used to mark late endosomes and lysosomes (hereafter: [endo]lysosomes) in *Drosophila*,[27,31,36,40-42] highlighted (endo)lysosomes after 4 h of starvation in the 3rd instar fat body (Fig. 2A). In contrast, the sensor remained diffusely distributed at this time-point (Fig. 2A''). However, similar to mammalian cells,[28] sensor puncta largely colocalized with (endo)lysosomes after prolonged starvation (Fig. 2B). Quantitative analysis revealed that 87% ± 4% of the biosensor puncta colocalized with (endo)lysosomes at 25 hps (Fig. 3K; 5 fields of view; n = 32 cells, total puncta = 708). Consistent with these results, LysoSensor Green staining to label acidic compartments including late endosomes and lysosomes in photoactivated and starved (25 hps) live L3 fat body also revealed significant overlap with the reporter puncta (Fig. 2C).

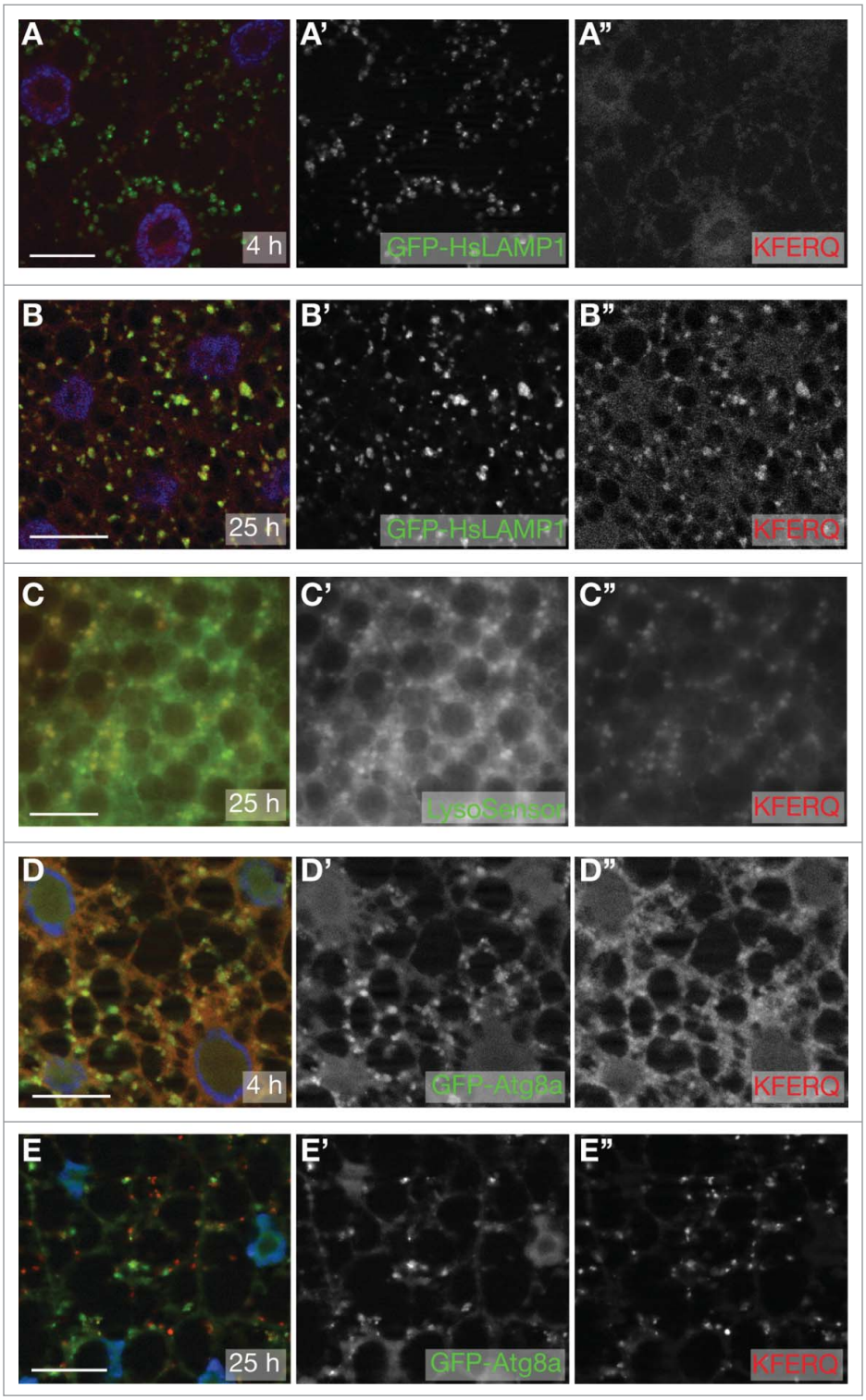

Figure 2. Biosensor puncta colocalize with (endo)lysosomes. (A to C) While at 4 hps the sensor remains diffusely distributed in the cytoplasm (A), at 25 hps the sensor forms puncta that strongly colocalize with a GFP-HsLAMP1 fragment used to mark (endo)lysosomes (B; see Figure 3K for quantification). (C) Sensor puncta strongly colocalize with acidic compartments stained with LysoSensor Green dye in live fat body tissue at 25 hps. (D and E) While a robust formation of autophagosomes marked by GFP-Atg8a is detected at 4 hps (D, D′), the KFERQ sensor remains diffusely distributed in the fat body (D″). At 25 hps (E), some autophagosomes (E′) overlap with biosensor puncta (E″; see Fig. 3K for quantification). Monochrome images show the indicated channels. A: confocal images; C: epifluorescence image; B, D, E: ApoTome images. Scale bars: 20 μm.

Next we characterized the biosensor puncta relative to autophagosomes and endosomes. GFP fused to Atg8a, a *Drosophila* ortholog of LC3, marks autophagosomes[36] and, as previously reported accumulated in autophagosomes at 4 hps, indicating robust MA,[27,36,37] while the biosensor remained diffuse (Fig. 2D). Upon prolonged starvation, 29% ± 12% of reporter puncta colocalized with GFP-Atg8a, likely reflecting lysosomes or late endosomes that had previously fused with autophagosomes (Fig. 2E; quantification in Fig. 3K, 10 fields of view, n = 40 cells, 1817 puncta). These data again show that formation of

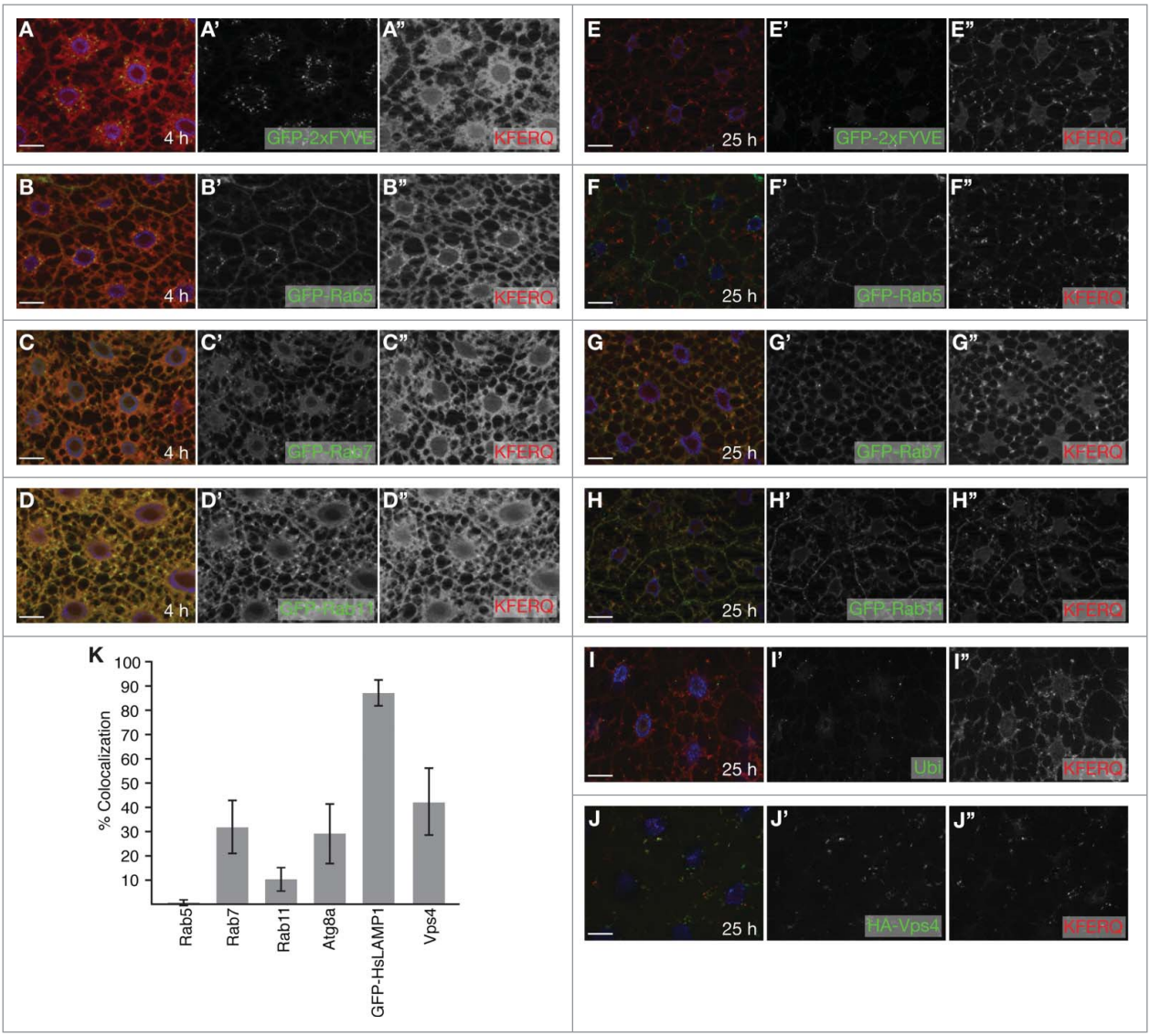

Figure 3. Colocalization of the biosensor with endosomal markers. (A to D) Early endosomes marked by GFP-2xFYVE or GFP-Rab5 (A and B, respectively), late endosomes (GFP-Rab7; C), and recycling endosomes (GFP-Rab11; D) show localization distinct from the diffuse pattern of the biosensor 4 hps. (E to H) At 25 hps, no colocalization of the sensor puncta is detected with early endosomes (E and F). Little colocalization is found with recycling endosomes (G), while 31% of the sensor signal colocalizes with late endosomes (H). (I) Antibody staining for ubiquitin and the biosensor show that the sensor puncta are not due to nonspecific protein aggregates. (J) Antibody staining revealed strong colocalization of reporter puncta with HA-VPS4. (K) Quantification of percentage of colocalization of biosensor puncta with the indicated markers after prolonged starvation (mean percentages ± STDV). Monochrome images show the indicated channels (ApoTome). Scale bars: 20 μm.

biosensor puncta is temporally distinct from MA activation and that they initiate in different vesicular compartments.

We then performed quantitative colocalization studies of the reporter puncta with respect to early endosomes (GFP-2xFYVE, GFP-Rab5),[36,43] recycling endosomes (GFP-Rab11),[44] and late endosomes (GFP-Rab7).[45] At 4 hps, GFP-2xFYVE (Fig. 3A) and GFP-Rab5 (Fig. 3B) showed the expected perinuclear puncta,[36] and both GFP-Rab7 (Fig. 3C) and GFP-Rab11 (Fig. 3D) formed cytoplasmic puncta, which were distinct from the uniformly diffuse localization of the KFERQ-biosensor. At 25 hps, the reporter puncta did not colocalize with the perinuclear early endosomal markers (Figs. 3E and 3F for GFP-2xFYVE and GFP-Rab5, respectively; quantified in Fig. 3K for Rab5: 0.8% ± 0.8%, 1266 puncta in 40 cells) and showed only minimal overlap with the recycling endosomal marker GFP-Rab11 (10% ± 5%; Fig. 3H; quantified in Fig. 3K, 10 fields of view, 40 cells, 2071 puncta). In contrast, 31% ± 11% of the reporter puncta colocalized with GFP-Rab7 (Fig. 3G; quantified in Fig. 3K, 10 fields of view, 40 cells, 1406 puncta), a marker of the late endosomal compartment. Importantly, the lack of colocalization of the biosensor with ubiquitin (Fig. 3I) indicates that the discrete biosensor puncta are not due to aggregation of the fluorescent protein directly in the cytosol.

Formation of biosensor puncta is independent of macroautophagy

Starvation induced MA in 3rd instar fat body is evident within 1 hps and peaks at 4 hps.[27,35,46] Although we found no sensor puncta at 4 hps, a notable overlap between our biosensor and the autophagosomal marker GFP-Atg8a was detected at 25 hps (Figs. 2 and 3K). To genetically determine if sensor puncta formation requires MA, we assessed the sensor behavior in the absence of MA. The E1-like enzyme Atg7 is required to catalyze

Atg8 and Atg12 conjugation during starvation-induced autophagosome formation in the *Drosophila* fat body.[34,35] Compared to control, RNAi-mediated knockdown of *atg7* at 4 hps prevented formation of GFP-Atg8a-marked autophagosomes (Figs. S2A and S2B), but did not affect sensor puncta formation at 25 hps (Fig. 4A). To confirm this result, we induced homozygous mutant clones of the strong loss-of-function allele[35] $atg7^{d4}$ allowing us to compare mutant alongside wild-type tissue. We found that biosensor puncta formed in $atg7^{d4}$ mutant cells (marked by the absence of GFP in Fig. 4B) upon prolonged starvation. Quantification showed similar numbers of puncta in mutant and wild-type cells (puncta ratio of mutant to wild type = 0.95±0.1; 37 cells), clearly indicating that this essential MA gene is dispensable for KFERQ-sensor puncta formation. Similarly, knockdown of *atg5* and *atg12* using RNAi knockdown lines that have previously been established to inhibit MA in the *Drosophila* fat body or midgut[34,42] (see also Fig. S2D) has no effect on KFERQ-sensor puncta formation (Fig. 4C for $atg5^{IR\ JF02703}$ and Figs. 4D, E for $atg12^{IR\ JF02704}$ and $atg12^{IR\ HMS01153}$, respectively), clearly demonstrating that sensor puncta formation is not only temporally, but also genetically distinct from MA.

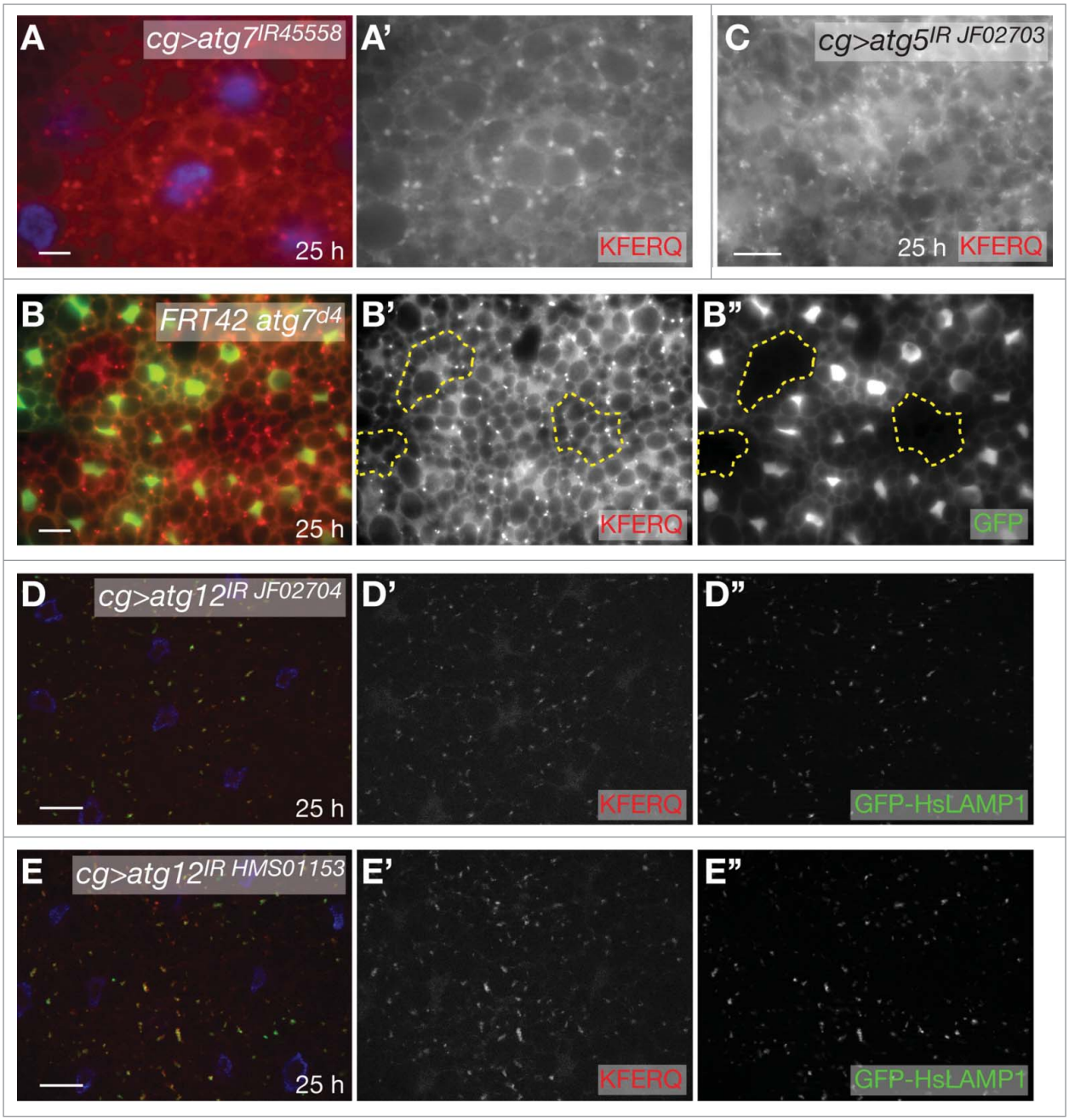

Figure 4. Biosensor puncta form in the absence of macroautophagy. (A and B) RNAi-mediated knockdown of *atg7* (A) or lack of *atg7* in $atg7^{d4}$ mutant clones (B; compare homozygous mutant tissue marked by the absence of GFP (B″) and outlined in yellow dotted lines with surrounding wild-type tissue) show that *atg7* is dispensable for sensor puncta formation. (C to E) Knockdown of *atg5* (C) or *atg12* (D and E) using the indicated RNAi lines show that neither *atg5* nor *atg12* is required for sensor puncta formation upon prolonged starvation. In (D, E), (endo)lysosomes are marked using GFP-HsLAMP1. Monochrome images show the indicated channels. A, C: epifluorescence; B, D, E: ApoTome. Scale bars: 20 μm.

Drosophila has an endosomal microautophagy-like pathway

In mammals, the cytosolic chaperone HSPA8 contributes to CMA and eMI pathways by binding the KFERQ-targeting motif of substrates,[17] and in the latter case mediating endosomal membrane recruitment.[21] The *Drosophila* genome encodes 6 Hsc70 paralogs with Hsc70-4 being the most similar to human HSPA8 (87% sequence identity). To determine whether Hsc70-4, in addition to its known function in endocytosis,[47] is also required for KFERQ-reporter puncta formation in *Drosophila*, we used 2 independent, nonoverlapping dsRNAi lines targeting *Hsc70-4* to knock down the chaperone in the fat body. At 25 hps, knockdown of *Hsc70-4* caused loss of biosensor puncta, while GFP-HsLAMP1-positive (endo)lysosomes appeared unaffected (*Hsc70-4*^{IR50222} and *Hsc70-4*^{IR101734} in Figs. 5A and 5B, respectively). Similarly, mutant cells in mosaics of the null or strong hypomorphic *Hsc70-4*$^{\Delta 16}$ allele[47] are unable to form reporter puncta (Fig. 5C; compare mutant cells lacking GFP in 5C″ with wild-type neighbors), suggesting that, as in mammals, the *Drosophila* form of a KFERQ motif-dependent form of autophagy requires Hsc70-4.

Biochemical fractionation experiments in mammalian cells demonstrated that eMI, unlike CMA, depends on the ESCRT machinery.[21] The ESCRT machinery consists of 4 sequentially recruited multiprotein complexes (ESCRT 0 to III), which are required for MVB biogenesis,[48,49] although in the *Drosophila* eye disc epithelium, MVBs also can form in the absence of ESCRT 0.[50] To determine if we identified an eMI-like process in *Drosophila*, we tested ESCRT machinery contribution to biosensor puncta formation. We generated homozygous mutant clones in the fat body disrupting *Hrs*^{D28} *Stam*^{2L2896},[50] a core dimer of ESCRT 0 (Fig. 6A, B), *vps28*^{D2}, an ESCRT I member (Fig. 6C),[51] *vps25*^{A3} (Fig. 6D),[52] an ESCRT II component, and *vps32*^{G5} (Fig. 6E),[51] an ESCRT III complex factor. After prolonged starvation, mutant clones of the ESCRT I, II, and III lacked reporter puncta in a cell autonomous manner, while the surrounding wild-type cells formed puncta (Figs. 6C to E), illustrating biosensor puncta dependence on the ESCRT machinery. In contrast, we find that, consistent with MVBs being able to form in the absence of Hrs and Stam,[50] ESCRT 0 is not absolutely required for sensor puncta formation, as *Hrs Stam* double mutations were partially penetrant only and fat bodies contained mutant cells without or with puncta (compare Figs. 6A and 6B). Importantly,

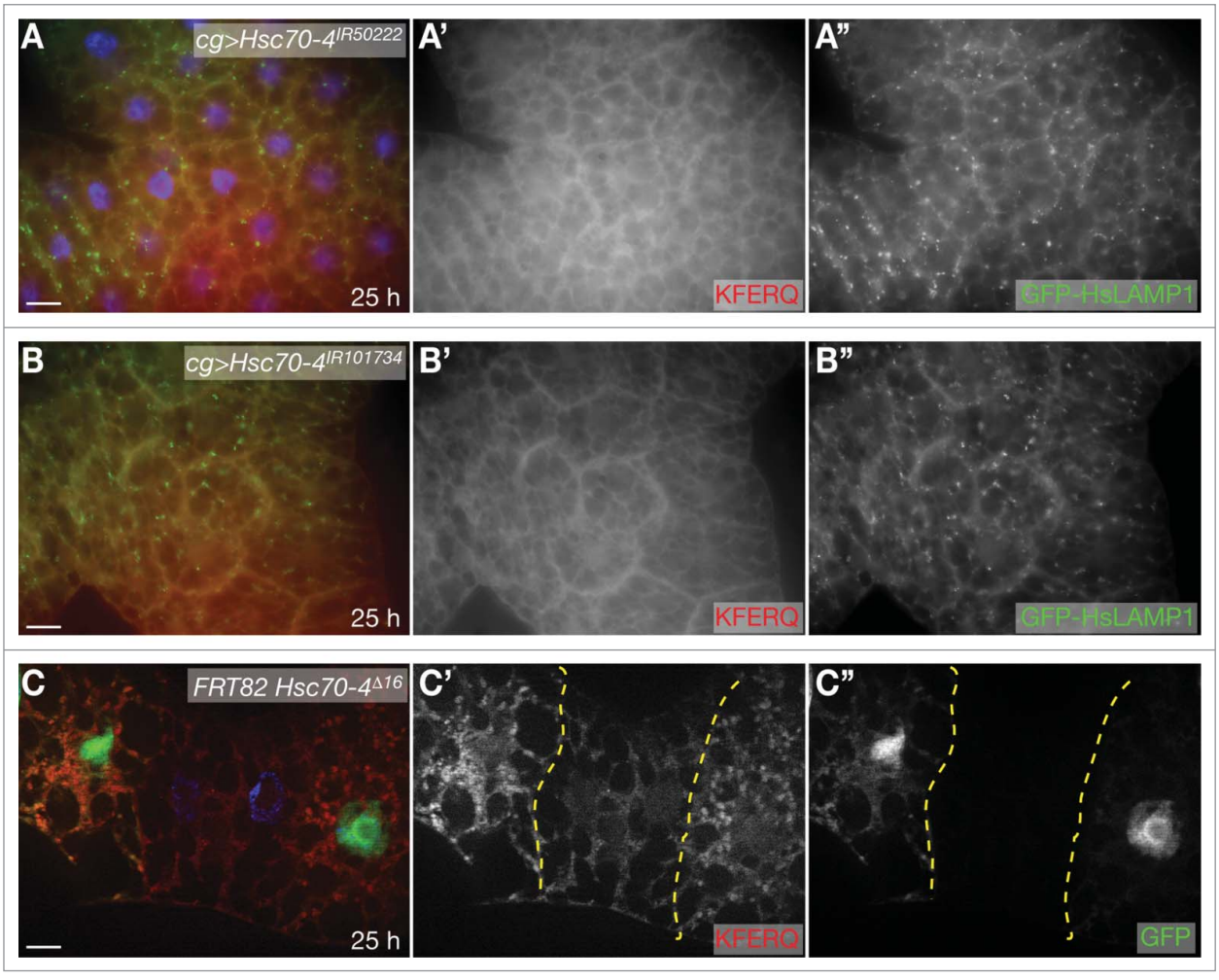

Figure 5. Requirement of the Hsc70-4 chaperone. (A and B) IR50222 (A) and IR101734 (B), 2 independent, nonoverlapping dsRNA hairpins used to knock down *Hsc70-4* prevent the formation of biosensor puncta after 25-h of starvation when expressed in the fat body (A′ and B′). Note that lysosomes remain present (A″ and B″). (C) Compared to wild-type cells, homozygous mutant cells in clones of the *Hsc70-4*$^{\Delta 16}$ allele (marked by the absence of GFP (C″) and outlined in yellow) lack sensor puncta (C′). Monochrome images on the right show the indicated channels. A, B: epifluorescence; C: ApoTome. Scale bars: 20 μm.

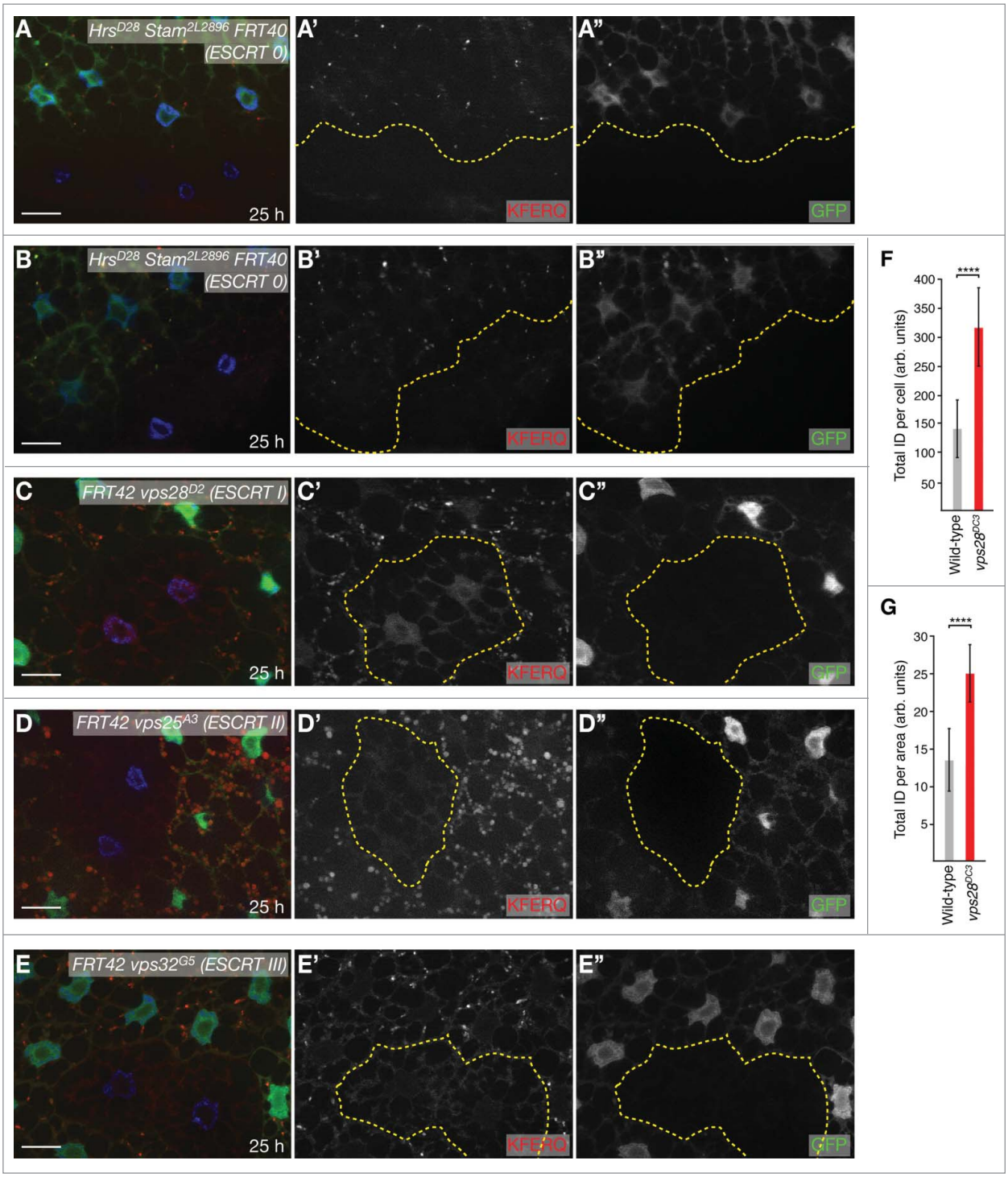

Figure 6. Biosensor puncta formation requires the ESCRT machinery. (A and B) The ESCRT 0 components Hrs and Stam contribute to, but are not essential for, sensor puncta formation, as homozygous double-mutant clones of *Hrs*^{D28} *Stam*^{2L2896} can lack sensor puncta (A) or not (B). (C to E) Cells mutant for *vps28*^{D2}, an ESCRT I component (C), *vps25*^{A3}, an ESCRT II component (D) or *vps32*^{G5}, an ESCRT III component (E) lack sensor puncta at 25 hps. Mutant clones are marked by the absence of GFP (A″ to E″) and outlined by a dotted yellow line. Monochrome images show the indicated channels (ApoTome). Scale bars: 20 μm. (F and G) The sensor is stabilized in cells mutant for the ESCRT I component *vps28*^{D2}, thus indicating that the ESCRT machinery is required for sensor degradation. Quantification of Integrated Density (ID) per cell (F) or area (G) both show that the total sensor signal in mutant cells (red bars) is significantly higher than in normal cells (gray bars; n = 10 cells per genotype; Student *t* test; ***, $P < 0.00001$; note that both ways of quantification are shown as mutant cells show a trend toward slightly increased size).

we quantified the reporter signal intensity of cells mutant for the ESCRT I component *vps28* compared to neighboring wild-type cells and found that, as expected if MVB formation is required for degradation of the reporter, the biosensor was statistically significantly-stabilized in the mutant cells (normalized per cell in Fig. 6F and per area in Fig. 6G).

Consistent with a MVB-dependent process, we also found a significant colocalization of the sensor puncta with Vps4, an ATPase required for dissociation of the ESCRT machinery upon pinching off of the intralumenal vesicles during MVB formation (Fig. 3J; quantified in Fig. 3K: 41.5%±14.2%; 1130 puncta in 43 cells).[48] To confirm localization of the reporter to

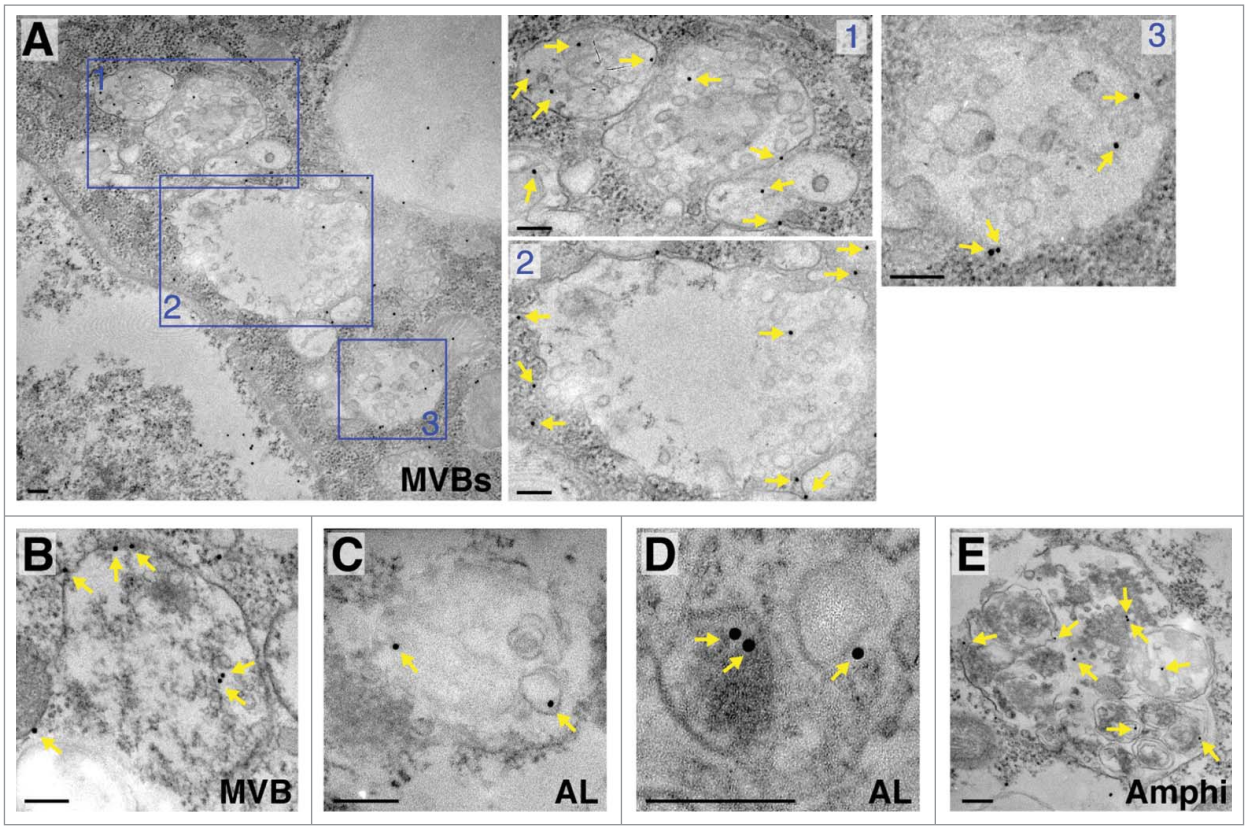

Figure 7. The KFERQ-sensor is present in multivesicular bodies. (A and B) Immunoelectron microscopy using anti-RFP antibodies shows gold particles (yellow arrows) decorating MVBs (areas outlined in blue in (A) are shown at higher magnification on the right. Additionally, the sensor can also be detected in autolysosomes (AL in C and D) and amphisomes (Amphi; E). 25 hps; scale bars: 200 nm.

MVBs, and demonstrate internalization into their lumen, we performed immuno-EM analysis of fat body cells starved for 25-h using anti-RFP antibodies. Fig. 7A and 7B show that the reporter indeed is found in MVBs, both associated to the membrane but also in the lumen. Additionally and consistent with the colocalization studies presented in Figs. 2 and 3, we detected reporter signals in the lumen of compartments with features indicative of active degradation and in those containing both small endocytic vesicles and cytosolic cargo, compatible with autolysosomes and amphisomes, respectively (Fig. 7C to E).

Taken together, the KFERQ-motif and starvation dependent reporter puncta thus reflect a *Drosophila* version of endosomal microautophagy.

Drosophila eMI is controlled by inactivation of Tor signaling

MTOR (mechanistic target of rapamycin [serine/threonine kinase]) signaling represses MA by phosphorylating the ULK1/Atg1 kinase, thus preventing autophagosome formation (reviewed in refs. 53, 54). Consequently, in many organisms including *Drosophila*,[24,27,31] inhibition of Tor by amino acid deprivation (i.e., starvation), mutation, or by using the pharmacological inhibitor rapamycin is sufficient to trigger MA. As *Drosophila* eMI is dependent on prolonged starvation (Fig. 1), we wondered whether repression of Tor signaling is involved in its initiation. Rearing photoactivated larvae expressing the eMI reporter in the presence of rapamycin led to a robust induction of puncta under fed conditions (Fig. 8A), suggesting that Tor signaling under nutrient-rich conditions indeed prevents eMI. Reducing Tor activity by mutating its activator, the small GTPase Rheb (Ras homolog enriched in brain), also induced eMI reporter puncta in a cell autonomous manner under fed conditions (compare mutant cells lacking GFP in Fig. 8B to neighboring wild-type cells). Similarly, overexpression of Tsc1 and Tsc2, a GTPase activating complex for Rheb and thus inhibitor of Tor, is sufficient to promote eMI under fed conditions (Fig. 8C; note that larval growth is delayed and cells are considerably smaller). As inhibition of Tor relieves Atg1 inhibition in turn triggering MA,[24,31,32,55] we tested whether Atg1 and its binding partner Atg13 were required for the induction of eMI. Reporter puncta were absent in mutant clones of the $atg13^{81}$ null allele[31] (Fig. 8D). Similarly, fat bodies in which RNAi was used to knockdown *atg13* (see Fig. S2C for effectivity) or $atg1^{56}$ failed to form reporter puncta upon prolonged starvation (Figs. S2E and 8E; note that [endo]lysosomes appeared normal upon *atg1* knockdown). Taken together, our data thus suggest that *Drosophila* eMI is triggered by inhibition of Tor signaling under nutrient poor conditions and that Atg1-Atg13 may have an additional novel function in mediating eMI activation.

Discussion

Macroautophagy is conserved from yeast to humans, while CMA is presumed to be restricted to mammals and possibly birds, due the absence of an identifiable LAMP2A, a splice

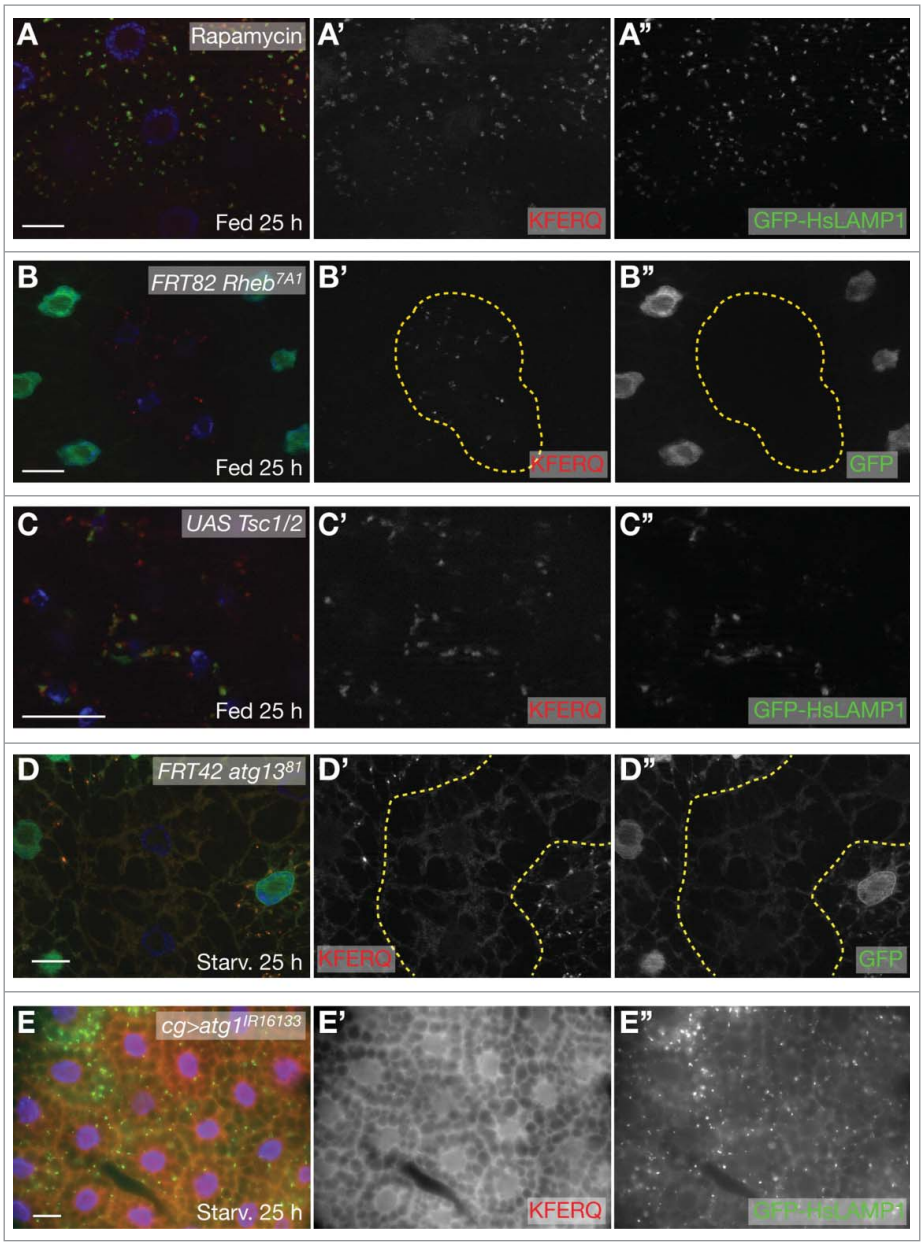

Figure 8. Tor signaling mediates the effects of starvation on *Drosophila* eMI. (A) Treatment of larvae with rapamycin to inhibit Tor induces eMI in *Drosophila* under fed conditions (notice robust puncta formation in A′). (B and C) Lack of the Tor activator Rheb in clones of $Rheb^{7A1}$ (B; mutant area indicated by lack of GFP; B″) or overexpression of the Tor inhibitors Tsc1/2 (C) is sufficient to promote eMI under fed conditions. (D) $atg13^{81}$ homozygous mutant tissue lacks biosensor puncta upon prolonged starvation (a mutant clone is marked by the absence of GFP in D″). (E) Knockdown of *atg1* prevents the formation of sensor puncta (E′) without affecting an (endo)lysosomal marker (E″). Yellow dotted lines outline homozygous mutant clones in (B, D). Monochrome images show the indicated channels. Scale bars: 20 μm.

isoform of LAMP2 that is limiting and essential for CMA,[18] in phylogenetically earlier species. The extent of conservation of microautophagy, the direct uptake of cytoplasmic components by membrane invaginations forming at the surface of either the vacuole (in yeast) or lysosomes and late endosomes (in mammals) remains elusive. Electron microscopy (EM) studies and in vitro reconstitution assays in yeast suggest that vacuoles can directly engulf or envelop cytoplasm or organelles for degradation (reviewed in ref. 12). MI also has been postulated to exist in mammalian cells based on EM images with apparent lysosomes engulfing cytoplasmic structures.[12] Recently, imaging and biochemical fractionation experiments in mammalian cells have revealed that late endosomes can selectively take up proteins with KFERQ-targeting motifs in addition to bulk cytoplasm.[21] This process, termed endosomal microautophagy (eMI), requires invagination of endosomes to form MVBs.[21] Using a KFERQ motif-containing biosensor, we found evidence for a selective autophagy process in a nonmammalian species in vivo. In *Drosophila* upon prolonged starvation, the biosensor localizes to LAMP1-positive compartments in a KFERQ and Hsc70-4 dependent manner, consistent with a CMA or eMI like process. Furthermore, localization to (endo)lysosomes is independent of *atg7, atg5*, and *atg12*, critical components of MA, but requires the ESCRT I (*vps28*), ESCRT II (*vps25*) and ESCRT III (*vps32*) complexes involved in formation of MVBs, consistent with eMI in mammals.[21]

In mammalian cells depleted of nutrients, induction of CMA peaks well after MA.[57-62] In our study, the biosensor behaves

analogously. In contrast to MA which is induced in the fat body within 1 h of amino-acid deprivation,[27] sensor puncta require starvation of longer than 12 h for induction and around 20 h for robust lysosomal localization. KFERQ-like motifs are relatively frequent with around 35% to 45% of proteins containing one in mammals and 43% in *Drosophila melanogaster*. Interestingly, in mammals, the KFERQ motif is required for protein targeting to CMA and eMI, but is only sufficient for CMA.[21,28] In contrast, our data show that in flies and distinct from mammals, the KFERQ motif is necessary and sufficient for biosensor targeting to eMI. The KFERQ motif is bound by the chaperone HSPA8 and is thus required for mammalian eMI and CMA.[17,19,21] We find a similar requirement for Hsc70-4, the most closely related *Drosophila* paralog for localization of the biosensor to lysosomal puncta. Our studies did not show binding of the KFERQ-PA-mCherry to Hsc70-4 in coimmunoprecipitation assays from larval tissue. Although it is possible that there is no direct association between the sensor and Hsc70 in flies, we favor the possibility that the available antibodies are not sensitive or efficient enough to detect such an interaction. A similar dependence on Hsc70-4 recently has been shown for the degradation of KFERQ-motif containing proteins in endosomes at synapses in *Drosophila* neuronal muscular junctions.[63] Furthermore, during eMI in mammals, HSPA8 mediates transport of cargo to endosomal membranes by binding to endosomal phosphatidylserine.[21] Consistently, it has recently been shown that Hsc70-4 has a membrane-deformation activity in *Drosophila* that is required for the control of synaptic protein turnover.[63] Although elimination of *Hsc70-4* is sufficient to disrupt eMI in *Drosophila*, we cannot discard the possibility that other *Drosophila Hsc70* paralogs may also contribute to this process. In particular, it would be interesting to investigate if all eMI-related functions that are performed by HSPA8, the single mammalian ortholog of the *Drosophila* Hsc70 family (i.e., substrate binding, targeting to endosomes and internalization into the forming vesicles) are all the task of *Drosophila Hsc70-4*, or if in flies any of these steps require another paralog.

In contrast to CMA, knockdown studies of the ESCRT I component TSG101 and the late acting VPS4[48,64] indicate that eMI requires components of the ESCRT machinery essential for the formation of MVBs.[21] Based on our results demonstrating that reporter puncta formation requires several components of the ESCRT machinery (Fig. 6) and our finding of the reporter in MVBs in immuno-EM (Fig. 7), we suggest that we identified and characterized a novel selective eMI-like process in the *Drosophila* fat body.

Our colocalization analyses revealed a close association of the biosensor with (endo)lysosomes (nearly 90% of the puncta overlap with GFP-HsLAMP1 or LysoSensor Green, a vital dye for acidic compartments),[27,31,36,40] consistent with studies of mammalian CMA for which the reporter originally was developed.[28] In flies, however, the sensor colocalizes more extensively with Atg8a (29%) and late endosomes (29%) compared to less than 10% in mammalian cells,[28] the latter consistent with transition of the sensor through late endosomes enroute to lysosomes. The greater colocalization of the sensor with GFP-Atg8a likely indicates convergence of MA and endocytic compartments in amphisomes [65] (also confirmed by our immuno-EM studies). Overall these findings further support that, in flies, the puncta report eMI instead of CMA.

Despite partial overlap between GFP-Atg8a and the sensor puncta, eMI in flies is independent of the core autophagy components *atg7, atg5*, and *atg12* (Fig. 4). Although autophagosomes have been described to form in the absence of the E1-like enzyme ATG7 in mouse embryonic fibroblasts [66] and in the *Drosophila* larval midgut, where Uba1 (ubiquitin-activating enzyme 1) exerts the function of Atg7,[34] *Drosophila atg7* mutant fat bodies show dramatically reduced formation of autophagosomes by morphological criteria in EM analyses and completely lack Atg8a (whose mammalian orthologs include LC3) reporter puncta (see refs. 34, 35 and Fig. S2B). These findings, and the temporally clearly distinct onset of MA during starvation (starting within 1 hps compared to >12 h for our biosensor; Fig. 1I),[27] strongly suggest that the process we identified in *Drosophila* is distinct from MA. Furthermore, autophagosomes increase in ESCRT mutant cells [37] in contrast to our sensor puncta that require the ESCRT machinery to form. Additionally, the independence of eMI of *atg7, atg5*, and *atg12* in flies suggests that this process is mechanistically distinct from forms of MI described in yeast, such as piecemeal microautophagy of the nucleus (PMN), which is dependent on *ATG* genes including *ATG7, ATG5*, and *ATG12* and micropexophagy, which is dependent on *ATG7* and *ATG5* (*ATG12* was not tested).[67,68] More recently, a Nbr1-mediated vacuolar targeting (NVT) pathway transporting certain hydrolases from the cytoplasm to the vacuole has been described in *S. pombe*.[69] While rather a transport or biogenic pathway than a degradation pathway, NVT shares genetic and topological similarities with the endosomal microautophagy described in mammals and the one we report here in flies. Uptake of the hydrolases by NVT depends on the ESCRT machinery, but is independent of MA genes including *ATG1, ATG5*, and *ATG13*. While it is unknown whether HSPA8/Hsc70 is required for NVT, substrate recognition appears to be mediated by Nbr1 and ubiquitination rather than a KFERQ motif, suggesting different mechanisms for biogenic and catabolic MVB-dependent pathways.

To date very little is known about the regulation of microautophagy. Starvation and refeeding experiments in mice showed that there is no evidence for food deprivation inducing MI; thus, MI is presumed to be a constitutive process in mammals.[70] In contrast, in *Drosophila*, eMI clearly can be induced by starvation (Fig. 1). During nutritional starvation, inactivation of Tor kinase leads to activation of the Atg1-Atg13 complex, which then acts as one of the triggers of MA.[24,31,32,71] Analogously, we showed that pharmacological or genetic inhibition of Tor signaling is sufficient to induce reporter puncta formation under nutrient-rich conditions (Fig. 8). Intriguingly and unknown for mammals, *Drosophila* eMI also depends on *atg13* and *atg1*, suggesting that that Tor inhibition may activate Atg1 and Atg13 during eMI. Atg1 and Atg13 may thus have an additional, late function in *Drosophila* to initiate eMI in addition to triggering autophagosome formation. If so, future experiments will have to address the mechanistic basis of eMI activation compared to MA.

The different requirements for starvation on the induction of MI in mammals and flies may be due to differences in the cell types assessed. However, it is equally tempting to speculate

that *Drosophila* eMI is an older form of selective autophagy that fulfills functions that in mammals are shared between eMI (likely the constitutive form) and CMA (the starvation-induced variant). Identification of eMI in a genetically tractable model organism allows future studies to address how starvation triggers eMI in flies and to identify novel components required for this process.

Materials and methods

Fly strains and genetics

r4-Gal4, fb-Gal4, cg-Gal4, yw hsflp;UAS-GFP-ATG8a,[36] *UAS-GFP-2xFYVE*,[36] *hsflp; cg-Gal4 FRT42D UAS-GFPnls, hsflp; r4-Gal4 FRT82B UAS-GFPnls, FRT42 atg7*^{d4},[35] and *FRT82B atg13*^{81}*/TM6B* were kind gifts of Dr. T. Neufeld (University of Minnesota).[31] *UAS-GFP-Rab5/CyO*, and *UAS-Rab7-GFP/CyO* were gifts of Dr. M. Gonzalez Gaitan (University of Geneva, Switzerland).[43,45] *FRT82 Hsc70-4*$^{\Delta 16}$ is a null allele or strong hypomorph[72] and was a kind gift or Dr. Henry Chang (Purdue University). *UAS-Rab11-GFP*, and *UAS-GFP-HsLAMP1/CyO; Sb-boss1/TM6B* were gifts of Drs. G. Davis (UCSF, CA, USA) and T. E. Rusten (Oslo University Hospital, Norway), respectively,[27,40] and *Hrs*^{D28} *Stam*^{2L2896} *FRT40A*,[50] *FRT vps28*^{D2}, *FRT42D vps25*^{A3}*/CyO twist-Gal4-UAS-GFP* and *FRT42D vps32 (aka shrub)*^{G5}*/CyO twist-Gal4-UAS-GFP* were gifts from T. Vaccari (IFOM-IEO Campus, Italy).[51,52] *UAS-Tsc1-tsc2* (aka *gigas*), and *FRT82 Rheb*^{7A1} were a kind gift of Dr. H. Stocker (ETH, Switzerland).[73] Additional strains are described in FlyBase. VDRC-16133 (*atg1*), VDRC-45558 (*atg7*), VDRC-27956 (*atg13*), VDRC-50222 and VDRC-101734 (*Hsc70-4*) were from the VDRC collection.[74] TRiP-JF02703 (*atg5*; BL-27551), TRiP-JF02704 (*atg12*; BL-27552), TRiP-HMS01153 (*atg12*; BL-34675) lines were obtained from the Bloomington stock center.[75] *UAS-HA-Vps4/CyO* was a kind gift of Dr. J. Treisman (NYU, NY, USA) and rescues a *vps4* loss-of-function mutation (J. Treisman, personal communication).[76]

The GFP-marked mutant clones were generated by FLP/FRT mitotic recombination using hsFLP.[77] Embryos were collected after 6 to 8 h of egg-laying, followed by 1.5-h heat shock treatment at 37°C. For comparison of reporter puncta in wild-type cells and *atg7* mutant clones, 7 fields of view and a total 37 cells were analyzed.

Plasmids and transgenic flies

pPA_KFEAA_mCherry was made by replacing the NheI/BamHI fragment of pPA_KFERQ_mCherry[28] with annealed oligonucleotides KFEAAmutUpper (CTAGCGCCACCATGAAGGAAACTGCAGCAGCCAAGTTTGAGGCGGCGCACATGGACTCCAGCACTTCCGCTGCG) and KFEAAmutLower (GATCCGCAGCGGAAGTGCTGGAGTCCATGTGCGCCGCCTCAAACTTGGCTGCTGCAGTTTCCTTCATGGTGGCG). pUAST_KFERQ_PAmCherry and pUAST_KFEAA_PAmCherry were made by cloning the NheI (blunt)/NotI fragments of pPA_KFERQ_mCherry and pPA_KFEAA_mCherry, respectively, into the EcoRI (blunt)/NotI sites of pUAST. pUAST_PAmCherryN1 was made by cloning the NheI(blunt)/BglII fragment of pPA_mCherryN1 into the EcoRI(blunt)/BglII site of pUAST.

Embryo injections were performed by Rainbow Transgenic Flies (Camarillo, CA, USA) and balanced using standard procedures.

Western analysis

For western analysis, 20 3rd instar larvae were washed twice in phosphate-buffered saline (PBS; Corning Cellgro, 55-031-PC) and lysed in 250 μl RIPA buffer (20 mM Tris, pH 8.0, 150 mM NaCl, 5 mM EDTA, 1% IGEPAL R CA-630 [Fisher, ICN19859650], 0.25% deoxycholate [United States Biological, D3180], 1 μM pepstatin [Fisher, BP2671-10], 10 μM leupeptin [Fisher, BP2662-25], 1 mM benzamidine [Fisher BP435-25]) with a motorized pestle. After centrifugation for 10 min at 10,000 g at 4°C, 200 μl of the supernatant fraction was transferred to fresh tubes. Protein concentration was determined using a Lowry assay[78] and 100 μg protein were loaded on a 12% SDS PAGE gel and processed for western analysis using standard procedures.[79] Rabbit anti-RFP[80] was used at 1:10,000 (a kind gift of Dr. E. Snapp, Albert Einstein College of Medicine, Bronx, NY, USA).

Photoactivation of sensor in larvae

Ten to 12 virgins (e.g. *UAS-KFERQ-PA-mCherry; cgGal4/ S:T*) were mated to 10 appropriate males for 1 d using standard *Drosophila* culture conditions. After 4 d, 40 to 60 late 2nd instar and early 3rd instar larvae were separated from food and washed twice with H_2O. Larvae were transferred to a 35-mm culture dish containing 800 μl Graces insect medium (Invitrogen, 11605-094) with 10% heat-inactivated fetal bovine serum (Atlanta Biochemicals, S11050). The PA-cherry sensor was photoactivated by exposure to a 405-nm light source for 11 min (at 2.8 A, approximately 60 μW/cm^2; see also ref. 28.) Immediately after photoactivation, larvae were washed 3 times with H_2O and transferred to 35-mm dishes with small filter papers soaked in 20% sucrose (Fisher, BP220-1) solution (for starvation) or 20% sucrose solution with heat killed yeast paste (Lab Scientific, Fly-8040-10; fed conditions).[27] Larvae were kept in the dark and checked for dead larvae (which were removed) after a few hours. Generally, surviving larvae developed to morphologically normal adults.

After the desired time, larvae were washed twice in H_2O, cut open and turned inside out for fixation in freshly made 4% paraformaldehyde in 1xPBS for 1 h at room temperature or overnight at 4°C. The larvae were then washed 3 times for 15 min and transferred to a microscope slide in a drop of mounting medium (DAPI fluoromount-G; Southern Biotech, 0100-20) and nonfat body tissue was removed. Fat bodies were imaged using a 63x 1.4 NA oil objective on either a Zeiss Axiovision epifluorescence microscope (Zeiss AxioVs40 V 4.8.2.0, Carl-Zeiss, Oberkochen, Germany), an ApoTome.2 system (Carl-Zeiss, Oberkochen, Germany) using an Axiovert 200 (Carl-Zeiss, Oberkochen, Germany), or a Leica SP2-AOBS point laser scanning confocal microscope (Leica, Buffalo Grove, IL USA).

To inhibit Tor signaling, larvae were treated with 2 μM rapamycin (Calboichem, 553210) in 20% sucrose with heat killed yeast.[31]

Immunohistochemistry, reporter quantification, and colocalization analysis

Larvae were washed thoroughly in water, cut open and turned inside out to fix the carcass in freshly made 4% paraformaldehyde in 1xPBS for 1 h at room temperature or overnight at 4°C. Immunohistochemistry was performed following a standard protocol.[81] Primary antibodies used were mouse anti-ubiquitin (Cell Signaling Technology, P4D1; 1:300), rat anti-RFP (Chromotek, 5F8; 1:300), rat anti-HA (Roche 3F10, 12158167001; 1:250), and rabbit anti-RFP[80] (1:1000, a kind gift of Dr. E. Snapp). Secondary antibodies from Life Technologies (anti-mouse Alexa Fluor 488 [A11029], anti-rat Alexa Fluor 488 [A11006], anti-rat Alexa Fluor 568 [A11077], and anti-rabbit Alexa Fluor 568 [A11036]) were used at 1:300. For LysoSensor Green staining, fat bodies from appropriate larvae were dissected in PBS and incubated in 100 μM LysoSensor Green (Molecular Probes, DND-189) for 2 min. The stained fat body lobes were then immediately mounted in 60% glycerol-PBS and imaged.

Reporter signals were quantified from images taken under identical conditions using Fiji/ImageJ software (NIH). Briefly, the channels were split, separately thresholded for total signal and for puncta and the integrated Density (ID) was measured. As most of the signal is cytosolic, we either report total signal or puncta only. For single cell analyses, cells were outlined, the outside cleared, and the area measured. The image was then split into channels and the ID determined as above. Quantification for the colocalization analysis was performed using Fiji/ImageJ software (NIH) using individual frames after adjusting thresholds. The total number of green and red puncta were calculated with the 'Particle Analyzer' and 'Green and red puncta colocalization' (D. J. Swiwarski modified by R. K. Dagda) plugins in Macros (Fiji/ImageJ). Colocalization (%) was calculated using JACoP plugin of Fiji/ImageJ using the merged images in each case. The results were expressed as mean values ± STDV. Statistical analyses (One-way ANOVA with the Tukey post hoc test) were performed using Prism 6.

Transmission electron microscopy and immunogold labeling

Larvae were starved for 25-h (without photoactivation) and fat bodies were dissected and fixed in 1% glutaraldehyde and 4% paraformaldehyde in 0.1 M sodium cacodylate buffer, pH 7.4 at RT for 1 h. The fat pellet was then rinsed in sodium cacodylate buffer and postfixed to fix lipids in 1% aqueous osmium tetroxide, dehydrated through a graded series of ethanol, and embedded in LR White resin (Electron Microscopy Sciences, 14382). Ultrathin sections were cut on a Leica Ultracut 6 (Buffalo Grove, IL USA) and mounted on 200-mesh nickel grids. Immunogold labeling was performed using antigen-retrieval using sodium metaperiodate followed by washing in 50 mM glycine in PBS, blocking, and labeling with rabbit anti-RFP (1:500)[80] for 2 h. Samples were then washed extensively and incubated with the gold-conjugated secondary antibody (1:100; Electron Microscopy Sciences, 25109) for 2 h. After extensive washing, the grids were fixed a second time for 15 min in 2% glutaraldehyde, washed and negatively stained with 1% uranyl acetate for 15 min. All grids were viewed on a Joel 1200EX transmission electron microscope at 80 kV (Peabody, MA, USA).

Abbreviations

atg	autophagy related
CMA	chaperone-mediated autophagy
EM	electron microscopy
eMI	endosomal microautophagy
ESCRT	endosomal sorting complexes required for transport
GFP	green fluorescent protein
hps	hours poststarvation
Hsc	heat shock cognate protein
LAMP2A	lysosomal-associated membrane protein 2A
L3	3rd instar larva
MAP1LC3/LC3	microtubule-associated protein 1 light chain 3
MA	macroautophagy
MI	microautophagy
MVB	multivesicular body
PA	photoactivatable
Tor	target of rapamycin (serine/threonine kinase)
Tsc	Tuberous Sclerosis Complex
uba	ubiquitin-activating enzyme

Disclosure of potential conflicts of interest

No potential conflicts of interest were disclosed.

Acknowledgments

We thank Drs. T.P. Neufeld (University of Minneapolis), T.E. Rusten (Oslo University Hospital, Norway), J. Treisman (NYU Medical School), M. Gonzalez Gaitan (University of Geneva, Switzerland), G. Davis (UCSF), H. Stocker (ETH, Switzerland) and T. Vaccari (IFOM-IEO Campus, Italy), E. Snapp (Einstein) for plasmids, antibodies, fly strains, and advice. We also thank the TRiP at Harvard Medical School, VDRC and Bloomington stock collections for additional fly strains. We thank the Einstein Analytical Imaging Facility for microscope use. We would like to thank Drs. F. Marlow, C. Pfleger, and T.E. Rusten for critically reading the manuscript.

Funding

The project was funded by pilot grants of the Resnick Gerontology Center (9526-9944) and the Marion Bessin Liver Pathobiology and Gene Therapy Research Core Center (5P30DK41296 PI Shafritz), and NIA R21AG046805-01A1 (to AJ) and NIH AG031782 and DK098408 (to AMC). AM was the recipient of an Ellison Foundation/AFAR Postdoctoral Fellowship. The authors declare no conflict of interest.

References

[1] Levine B, Kroemer G. Autophagy in the pathogenesis of disease. Cell 2008; 132:27-42; PMID:18191218; http://dx.doi.org/10.1016/j.cell.2007.12.018

[2] Mizushima N, Levine B. Autophagy in mammalian development and differentiation. Nature cell biology 2010; 12:823-30; PMID:20811354; http://dx.doi.org/10.1038/ncb0910-823

[3] Wang CW, Klionsky DJ. The molecular mechanism of autophagy. Mol Med 2003; 9:65-76; PMID:12865942

[4] Vellai T, Takacs-Vellai K. Regulation of protein turnover by longevity pathways. Adv Exp Med Biol 2010; 694:69-80; PMID:20886758; http://dx.doi.org/10.1007/978-1-4419-7002-2_7

[5] Mizushima N, Levine B, Cuervo AM, Klionsky DJ. Autophagy fights disease through cellular self-digestion. Nature 2008; 451:1069-75; PMID:18305538; http://dx.doi.org/10.1038/nature06639

[6] Rubinsztein DC, Gestwicki JE, Murphy LO, Klionsky DJ. Potential therapeutic applications of autophagy. Nat Rev Drug Discov 2007; 6:304-12; PMID:17396135; http://dx.doi.org/10.1038/nrd2272

[7] Cuervo AM, Bergamini E, Brunk UT, Droge W, Ffrench M, Terman A. Autophagy and aging: the importance of maintaining "clean" cells. Autophagy 2005; 1:131-40; PMID:16874025; http://dx.doi.org/10.4161/auto.1.3.2017

[8] Rubinsztein DC, Marino G, Kroemer G. Autophagy and aging. Cell 2011; 146:682-95; PMID:21884931; http://dx.doi.org/10.1016/j.cell.2011.07.030

[9] Gelino S, Hansen M. Autophagy - An Emerging Anti-Aging Mechanism. J Clin Exp Pathol 2012; Suppl 4; PMID:23750326

[10] Arias E, Cuervo AM. Chaperone-mediated autophagy in protein quality control. Curr Opin Cell Biol 2011; 23:184-9; PMID:21094035; http://dx.doi.org/10.1016/j.ceb.2010.10.009

[11] Kaushik S, Cuervo AM. Chaperone-mediated autophagy: a unique way to enter the lysosome world. Trends Cell Biol 2012; 22:407-17; PMID:22748206; http://dx.doi.org/10.1016/j.tcb.2012.05.006

[12] Mijaljica D, Prescott M, Devenish RJ. Microautophagy in mammalian cells: revisiting a 40-year-old conundrum. Autophagy 2011; 7:673-82; PMID:21646866; http://dx.doi.org/10.4161/auto.7.7.14733

[13] Mizushima N, Noda T, Yoshimori T, Tanaka Y, Ishii T, George MD, Klionsky DJ, Ohsumi M, Ohsumi Y. A protein conjugation system essential for autophagy. Nature 1998; 395:395-8; PMID:9759731; http://dx.doi.org/10.1038/26506

[14] Ichimura Y, Kirisako T, Takao T, Satomi Y, Shimonishi Y, Ishihara N, Mizushima N, Tanida I, Kominami E, Ohsumi M, et al. A ubiquitin-like system mediates protein lipidation. Nature 2000; 408:488-92; PMID:11100732; http://dx.doi.org/10.1038/35044114

[15] Kirisako T, Ichimura Y, Okada H, Kabeya Y, Mizushima N, Yoshimori T, Ohsumi M, Takao T, Noda T, Ohsumi Y. The reversible modification regulates the membrane-binding state of Apg8/Aut7 essential for autophagy and the cytoplasm to vacuole targeting pathway. J Cell Biol 2000; 151:263-76; PMID:11038174; http://dx.doi.org/10.1083/jcb.151.2.263

[16] Dice JF. Peptide sequences that target cytosolic proteins for lysosomal proteolysis. Trends Biochem Sci 1990; 15:305-9; PMID:2204156; http://dx.doi.org/10.1016/0968-0004(90)90019-8

[17] Chiang HL, Terlecky SR, Plant CP, Dice JF. A role for a 70-kilodalton heat shock protein in lysosomal degradation of intracellular proteins. Science 1989; 246:382-5; PMID:2799391; http://dx.doi.org/10.1126/science.2799391

[18] Cuervo AM, Dice JF. A receptor for the selective uptake and degradation of proteins by lysosomes. Science 1996; 273:501-3; PMID:8662539; http://dx.doi.org/10.1126/science.273.5274.501

[19] Agarraberes FA, Terlecky SR, Dice JF. An intralysosomal hsp70 is required for a selective pathway of lysosomal protein degradation. J Cell Biol 1997; 137:825-34; PMID:9151685; http://dx.doi.org/10.1083/jcb.137.4.825

[20] Salvador N, Aguado C, Horst M, Knecht E. Import of a cytosolic protein into lysosomes by chaperone-mediated autophagy depends on its folding state. J Biol Chem 2000; 275:27447-56; PMID:10862611

[21] Sahu R, Kaushik S, Clement CC, Cannizzo ES, Scharf B, Follenzi A, Potolicchio I, Nieves E, Cuervo AM, Santambrogio L. Microautophagy of cytosolic proteins by late endosomes. Dev Cell 2011; 20:131-9; PMID:21238931; http://dx.doi.org/10.1016/j.devcel.2010.12.003

[22] Leao AN, Kiel JA. Peroxisome homeostasis in Hansenula polymorpha. FEMS yeast research 2003; 4:131-9; PMID:14613877; http://dx.doi.org/10.1016/S1567-1356(03)00070-9

[23] Nair U, Klionsky DJ. Molecular mechanisms and regulation of specific and nonspecific autophagy pathways in yeast. J Biol Chem 2005; 280:41785-8; PMID:16230342; http://dx.doi.org/10.1074/jbc.R500016200

[24] Scott RC, Schuldiner O, Neufeld TP. Role and regulation of starvation-induced autophagy in the Drosophila fat body. Dev Cell 2004; 7:167-78; PMID:15296714; http://dx.doi.org/10.1016/j.devcel.2004.07.009

[25] Butterworth FM, Emerson L, Rasch EM. Maturation and degeneration of the fat body in the Drosophila larva and pupa as revealed by morphometric analysis. Tissue Cell 1988; 20:255-68; PMID:3136556; http://dx.doi.org/10.1016/0040-8166(88)90047-X

[26] Lee CY, Cooksey BA, Baehrecke EH. Steroid regulation of midgut cell death during Drosophila development. Dev Biol 2002; 250:101-11; PMID:12297099; http://dx.doi.org/10.1006/dbio.2002.0784

[27] Rusten TE, Lindmo K, Juhasz G, Sass M, Seglen PO, Brech A, Stenmark H. Programmed autophagy in the Drosophila fat body is induced by ecdysone through regulation of the PI3K pathway. Dev Cell 2004; 7:179-92; PMID:15296715; http://dx.doi.org/10.1016/j.devcel.2004.07.005

[28] Koga H, Martinez-Vicente M, Macian F, Verkhusha VV, Cuervo AM. A photoconvertible fluorescent reporter to track chaperone-mediated autophagy. Nat Commun 2011; 2:386; PMID:21750540; http://dx.doi.org/10.1038/ncomms1393

[29] Arquier N, Leopold P. Fly foie gras: modeling fatty liver in Drosophila. Cell Metab 2007; 5:83-5; PMID:17276349; http://dx.doi.org/10.1016/j.cmet.2007.01.006

[30] Deutsch J, Laval M, Lepesant JA, Maschat F, Pourrain F, Rat L. Larval fat body-specific gene expression in D. melanogaster. Developmental genetics 1989; 10:220-31; PMID:2500286; http://dx.doi.org/10.1002/dvg.1020100311

[31] Chang YY, Neufeld TP. An Atg1/Atg13 complex with multiple roles in TOR-mediated autophagy regulation. Mol Biol Cell 2009; 20:2004-14; PMID:19225150; http://dx.doi.org/10.1091/mbc.E08-12-1250

[32] Scott RC, Juhasz G, Neufeld TP. Direct induction of autophagy by Atg1 inhibits cell growth and induces apoptotic cell death. Curr Biol 2007; 17:1-11; PMID:17208179; http://dx.doi.org/10.1016/j.cub.2006.10.053

[33] Brand AH, Perrimon N. Targeted gene expression as a means of altering cell fates and generating dominant phenotypes. Development 1993; 118:401-15; PMID:8223268

[34] Chang TK, Shravage BV, Hayes SD, Powers CM, Simin RT, Wade Harper J, Baehrecke EH. Uba1 functions in Atg7- and Atg3-independent autophagy. Nature cell biology 2013; 15:1067-78; PMID:23873149; http://dx.doi.org/10.1038/ncb2804

[35] Juhasz G, Erdi B, Sass M, Neufeld TP. Atg7-dependent autophagy promotes neuronal health, stress tolerance, and longevity but is dispensable for metamorphosis in Drosophila. Genes Dev 2007; 21:3061-6; PMID:18056421; http://dx.doi.org/10.1101/gad.1600707

[36] Juhasz G, Hill JH, Yan Y, Sass M, Baehrecke EH, Backer JM, Neufeld TP. The class III PI(3)K Vps34 promotes autophagy and endocytosis but not TOR signaling in Drosophila. J Cell Biol 2008; 181:655-66; PMID:18474623; http://dx.doi.org/10.1083/jcb.200712051

[37] Rusten TE, Vaccari T, Lindmo K, Rodahl LM, Nezis IP, Sem-Jacobsen C, Wendler F, Vincent JP, Brech A, Bilder D, et al. ESCRTs and Fab1 regulate distinct steps of autophagy. Curr Biol 2007; 17:1817-25; PMID:17935992; http://dx.doi.org/10.1016/j.cub.2007.09.032

[38] Chiang HL, Dice JF. Peptide sequences that target proteins for enhanced degradation during serum withdrawal. J Biol Chem 1988; 263:6797-805; PMID:3360807

[39] Cuervo AM, Stefanis L, Fredenburg R, Lansbury PT, Sulzer D. Impaired degradation of mutant alpha-synuclein by chaperone-mediated autophagy. Science 2004; 305:1292-5; PMID:15333840; http://dx.doi.org/10.1126/science.1101738

[40] Pulipparacharuvil S, Akbar MA, Ray S, Sevrioukov EA, Haberman AS, Rohrer J, Kramer H. Drosophila Vps16A is required for trafficking to lysosomes and biogenesis of pigment granules. J Cell Sci 2005; 118:3663-73; PMID:16046475; http://dx.doi.org/10.1242/jcs.02502

[41] Mauvezin C, Ayala C, Braden CR, Kim J, Neufeld TP. Assays to monitor autophagy in Drosophila. Methods 2014; 68:134-9; PMID:24667416; http://dx.doi.org/10.1016/j.ymeth.2014.03.014

[42] Nagy P, Varga A, Kovacs AL, Takats S, Juhasz G. How and why to study autophagy in Drosophila: it's more than just a garbage chute. Methods 2015; 75:151-61; PMID:25481477; http://dx.doi.org/10.1016/j.ymeth.2014.11.016

[43] Wucherpfennig T, Wilsch-Brauninger M, Gonzalez-Gaitan M. Role of Drosophila Rab5 during endosomal trafficking at the synapse and evoked neurotransmitter release. J Cell Biol 2003; 161:609-24; PMID:12743108; http://dx.doi.org/10.1083/jcb.200211087

[44] Emery G, Hutterer A, Berdnik D, Mayer B, Wirtz-Peitz F, Gaitan MG, Knoblich JA. Asymmetric Rab 11 endosomes regulate delta recycling and specify cell fate in the Drosophila nervous system. Cell 2005; 122:763-73; PMID:16137758; http://dx.doi.org/10.1016/j.cell.2005.08.017

[45] Entchev EV, Schwabedissen A, Gonzalez-Gaitan M. Gradient formation of the TGF-beta homolog Dpp. Cell 2000; 103:981-91; PMID:11136982; http://dx.doi.org/10.1016/S0092-8674(00)00200-2

[46] Juhasz G, Neufeld TP. Experimental control and characterization of autophagy in Drosophila. Methods Mol Biol 2008; 445:125-33; PMID:18425447; http://dx.doi.org/10.1007/978-1-59745-157-4_8

[47] Chang HC, Newmyer SL, Hull MJ, Ebersold M, Schmid SL, Mellman I. Hsc70 is required for endocytosis and clathrin function in Drosophila. J Cell Biol 2002; 159:477-87; PMID:12427870; http://dx.doi.org/10.1083/jcb.200205086

[48] Fader CM, Colombo MI. Autophagy and multivesicular bodies: two closely related partners. Cell Death Differ 2009; 16:70-8; PMID:19008921; http://dx.doi.org/10.1038/cdd.2008.168

[49] Raiborg C, Stenmark H. The ESCRT machinery in endosomal sorting of ubiquitylated membrane proteins. Nature 2009; 458:445-52; PMID:19325624; http://dx.doi.org/10.1038/nature07961

[50] Tognon E, Wollscheid N, Cortese K, Tacchetti C, Vaccari T. ESCRT-0 is not required for ectopic Notch activation and tumor suppression in Drosophila. PLoS One 2014; 9:e93987; PMID:24718108; http://dx.doi.org/10.1371/journal.pone.0093987

[51] Vaccari T, Rusten TE, Menut L, Nezis IP, Brech A, Stenmark H, Bilder D. Comparative analysis of ESCRT-I, ESCRT-II and ESCRT-III function in Drosophila by efficient isolation of ESCRT mutants. J Cell Sci 2009; 122:2413-23; PMID:19571114; http://dx.doi.org/10.1242/jcs.046391

[52] Vaccari T, Bilder D. The Drosophila tumor suppressor vps25 prevents nonautonomous overproliferation by regulating notch trafficking. Dev Cell 2005; 9:687-98; PMID:16256743; http://dx.doi.org/10.1016/j.devcel.2005.09.019

[53] Dunlop EA, Tee AR. mTOR and autophagy: a dynamic relationship governed by nutrients and energy. Semin Cell Dev Biol 2014; 36:121-9; PMID:25158238; http://dx.doi.org/10.1016/j.semcdb.2014.08.006

[54] Russell RC, Yuan HX, Guan KL. Autophagy regulation by nutrient signaling. Cell research 2014; 24:42-57; PMID:24343578; http://dx.doi.org/10.1038/cr.2013.166

[55] Jung CH, Ro SH, Cao J, Otto NM, Kim DH. mTOR regulation of autophagy. FEBS letters 2010; 584:1287-95; PMID:20083114; http://dx.doi.org/10.1016/j.febslet.2010.01.017

[56] Denton D, Shravage B, Simin R, Mills K, Berry DL, Baehrecke EH, Kumar S. Autophagy, not apoptosis, is essential for midgut cell death in Drosophila. Curr Biol 2009; 19:1741-6; PMID:19818615; http://dx.doi.org/10.1016/j.cub.2009.08.042

[57] Fuertes G, Martin De Llano JJ, Villarroya A, Rivett AJ, Knecht E. Changes in the proteolytic activities of proteasomes and lysosomes in human fibroblasts produced by serum withdrawal, amino-acid deprivation and confluent conditions. Biochem J 2003; 375:75-86; PMID:12841850; http://dx.doi.org/10.1042/bj20030282

[58] Dice JF, Chiang HL, Spencer EP, Backer JM. Regulation of catabolism of microinjected ribonuclease A. Identification of residues 7–11 as the essential pentapeptide. J Biol Chem 1986; 261:6853-9; PMID:3700419

[59] Wing SS, Chiang HL, Goldberg AL, Dice JF. Proteins containing peptide sequences related to Lys-Phe-Glu-Arg-Gln are selectively depleted in liver and heart, but not skeletal muscle, of fasted rats. Biochem J 1991; 275(Pt 1):165-9; PMID:2018472; http://dx.doi.org/10.1042/bj2750165

[60] Cuervo AM, Knecht E, Terlecky SR, Dice JF. Activation of a selective pathway of lysosomal proteolysis in rat liver by prolonged starvation. Am J Physiol 1995; 269:C1200-8; PMID:7491910

[61] Massey AC, Kaushik S, Sovak G, Kiffin R, Cuervo AM. Consequences of the selective blockage of chaperone-mediated autophagy. Proc Natl Acad Sci U S A 2006; 103:5805-10; PMID:16585521; http://dx.doi.org/10.1073/pnas.0507436103

[62] Kaushik S, Massey AC, Mizushima N, Cuervo AM. Constitutive activation of chaperone-mediated autophagy in cells with impaired macroautophagy. Mol Biol Cell 2008; 19:2179-92; PMID:18337468; http://dx.doi.org/10.1091/mbc.E07-11-1155

[63] Uytterhoeven V, Lauwers E, Maes I, Miskiewicz K, Melo MN, Swerts J, Kuenen S, Wittocx R, Corthout N, Marrink SJ, et al. Hsc70-4 Deforms Membranes to Promote Synaptic Protein Turnover by Endosomal Microautophagy. Neuron 2015; 88:735-48; PMID:26590345; http://dx.doi.org/10.1016/j.neuron.2015.10.012

[64] Hurley JH, Emr SD. The ESCRT complexes: structure and mechanism of a membrane-trafficking network. Annual review of biophysics and biomolecular structure 2006; 35:277-98; PMID:16689637; http://dx.doi.org/10.1146/annurev.biophys.35.040405.102126

[65] Berg TO, Fengsrud M, Stromhaug PE, Berg T, Seglen PO. Isolation and characterization of rat liver amphisomes. Evidence for fusion of autophagosomes with both early and late endosomes. J Biol Chem 1998; 273:21883-92; PMID:9705327; http://dx.doi.org/10.1074/jbc.273.34.21883

[66] Nishida Y, Arakawa S, Fujitani K, Yamaguchi H, Mizuta T, Kanaseki T, Komatsu M, Otsu K, Tsujimoto Y, Shimizu S. Discovery of Atg5/Atg7-independent alternative macroautophagy. Nature 2009; 461:654-8; PMID:19794493; http://dx.doi.org/10.1038/nature08455

[67] Farre JC, Subramani S. Peroxisome turnover by micropexophagy: an autophagy-related process. Trends Cell Biol 2004; 14:515-23; PMID:15350980; http://dx.doi.org/10.1016/j.tcb.2004.07.014

[68] Krick R, Muehe Y, Prick T, Bremer S, Schlotterhose P, Eskelinen EL, Millen J, Goldfarb DS, Thumm M. Piecemeal microautophagy of the nucleus requires the core macroautophagy genes. Mol Biol Cell 2008; 19:4492-505; PMID:18701704; http://dx.doi.org/10.1091/mbc.E08-04-0363

[69] Liu XM, Sun LL, Hu W, Ding YH, Dong MQ, Du LL. ESCRTs Cooperate with a Selective Autophagy Receptor to Mediate Vacuolar Targeting of Soluble Cargos. Molecular cell 2015; 59:1035-42; PMID:26365378; http://dx.doi.org/10.1016/j.molcel.2015.07.034

[70] Mortimore GE, Hutson NJ, Surmacz CA. Quantitative correlation between proteolysis and macro- and microautophagy in mouse hepatocytes during starvation and refeeding. Proc Natl Acad Sci U S A 1983; 80:2179-83; PMID:6340116; http://dx.doi.org/10.1073/pnas.80.8.2179

[71] Dennis PB, Fumagalli S, Thomas G. Target of rapamycin (TOR): balancing the opposing forces of protein synthesis and degradation. Current opinion in genetics & development 1999; 9:49-54; PMID:10072357; http://dx.doi.org/10.1016/S0959-437X(99)80007-0

[72] Bronk P, Wenniger JJ, Dawson-Scully K, Guo X, Hong S, Atwood HL, Zinsmaier KE. Drosophila Hsc70-4 is critical for neurotransmitter exocytosis in vivo. Neuron 2001; 30:475-88; PMID:11395008; http://dx.doi.org/10.1016/S0896-6273(01)00292-6

[73] Stocker H, Radimerski T, Schindelholz B, Wittwer F, Belawat P, Daram P, Breuer S, Thomas G, Hafen E. Rheb is an essential regulator of S6K in controlling cell growth in Drosophila. Nature cell biology 2003; 5:559-65; PMID:12766775; http://dx.doi.org/10.1038/ncb995

[74] Dietzl G, Chen D, Schnorrer F, Su KC, Barinova Y, Fellner M, Gasser B, Kinsey K, Oppel S, Scheiblauer S, et al. A genome-wide transgenic RNAi library for conditional gene inactivation in Drosophila. Nature 2007; 448:151-6; PMID:17625558; http://dx.doi.org/10.1038/nature05954

[75] Ni JQ, Liu LP, Binari R, Hardy R, Shim HS, Cavallaro A, Booker M, Pfeiffer BD, Markstein M, Wang H, et al. A Drosophila resource of transgenic RNAi lines for neurogenetics. Genetics 2009; 182:1089-100; PMID:19487563; http://dx.doi.org/10.1534/genetics.109.103630

[76] Legent K, Liu HH, Treisman JE. Drosophila Vps4 promotes Epidermal growth factor receptor signaling independently of its role in receptor degradation. Development 2015; 142:1480-91; PMID:25790850; http://dx.doi.org/10.1242/dev.117960
[77] Xu T, Rubin GM. Analysis of genetic mosaics in developing and adult Drosophila tissues. Development 1993; 117:1223-37; PMID:8404527
[78] Lowry OH, Rosebrough NJ, Farr AL, Randall RJ. Protein measurement with the Folin phenol reagent. J Biol Chem 1951; 193:265-75; PMID:14907713
[79] Bjerrum OJ, Schafer-Nielsen C. Electrophoresis '86 proceedings of the Fifth Meeting of the International Electrophoresis Society. Weinheim, Germany: VCH Verlagsgesellschaft; 1986. Buffer systems and transfer parameters for semidry electroblotting with a horizontal apparatus.
[80] Chakrabarti O, Hegde RS. Functional depletion of mahogunin by cytosolically exposed prion protein contributes to neurodegeneration. Cell 2009; 137:1136-47; PMID:19524515; http://dx.doi.org/10.1016/j.cell.2009.03.042
[81] Jenny A, Darken RS, Wilson PA, Mlodzik M. Prickle and Strabismus form a functional complex to generate a correct axis during planar cell polarity signaling. The EMBO journal 2003; 22:4409-20; PMID:12941693; http://dx.doi.org/10.1093/emboj/cdg424